Hedonic representations in primary somatosensory cortices; Pain but not pleasure?

James H. Kryklywy*[a], Mana R. Ehlers[a,b], Andre O. Beukers[a,c], Sarah R. Moore[d,e], Rebecca M. Todd[a,f] & Adam K. Anderson[e]

[a]*Department of Psychology, University of British Columbia*

[b]*University Medical Centre, Hamburg-Eppendorf, [c]Department of Psychology, Princeton University, [d]Department of Medical Genetics, University of British Columbia, [e]Department of Human Development, Cornell University, [f]Djavad Mowafaghian Centre for Brain Health, University of British Columbia*

Abstract

In the somatosensory system, hedonic information is coded by mechanoreceptors at the point of contact. Pleasure and pain signals travel along peripheral nerve pathways distinct from those for discriminative touch. Yet it remains unknown whether the central nervous system represents tactile hedonic information in sensory cortices as another dimension of exteroceptive information, similar to discriminative touch signals, or if tactile hedonic information is instantiated in regions mediating internal interoceptive states. Employing representational similarity analysis with a new approach of pattern component modeling, we decomposed multivoxel patterns to demonstrate that signals of painful but not pleasurable touch are represented in primary somatosensory cortices. By contrast, all hedonic touch representations were identified in regions associated with affect and interoception. This suggests that touch should be divided into external-exteroceptive and internal-interoceptive dimensions, with hedonic touch represented as an internal state, even though evoked by external stimulation.

Introduction

Sensory experiences, such as embrace of a loved one or the pain of a stubbed toe, can be broken down into two central components: discrimination of the sensory information, and the associated hedonic response. The information processed by our sensory systems is typically viewed as objective, forming representations of a tangible external environment. In contrast, hedonic appraisal is regarded as a subjective centrally mediated process (Rolls, 2019; Todd et al., 2020), dependent on allocation of a mental common currency (McFarland and Sibly, 1975; Rolls, 2000) to estimate and compare affective value. However, there is evidence that hedonic valence (good vs bad) is coded by the peripheral afferents of the somatosensory system (Iggo, 1959, 1960; Vallbo et al., 1999) suggesting that aspects of tactile sensation are valenced from the point of contact (Miskovic and Anderson, 2018). It has been proposed that such valence discrimination in peripheral receptors contributes to internal representations of homeostatic threat and social safety (Craig, 2011, 2015). If these hedonic afferents reflect the internal physiological condition of the body more than external sensory events, then this would provide evidence for a unique dual role of our proximal senses. Consistent with Sherrington's classic distinction between exteroception and interoception (Sherrington, 1906) – sensation of an object in the external environment vs. the body itself as object – there may be unique and dissociable anatomical pathways underlying each, derived from stimulation of distinct tactile receptors (Kryklywy et al., 2020). To examine a neural dissociation between touch as an external object from the internal material self, we assessed whether tactile valence (pressure pain and social caress) is represented distinctly from discriminative touch, potentially reflecting distinct affective labelled lines residing outside of the traditional somatosensory cortices.

The somatosensory system contains multiple functional subsystems, with specific peripheral nerves serving as labeled-lines for information traveling into the central nervous system (McGlone and Reilly, 2010; McGlone et al., 2014). Fast large-diameter myelinated afferent fibers (A-fibers) support sensory discrimination. These fibers predominantly convey information about the timing and location of cutaneous sensory stimulation (McGlone and Reilly, 2010) with some fibers specialized for nociception (Nagi et al., 2019). Additional small-diameter unmyelinated afferent pathways (C-Fibers; Qiu et al., 2006) support the hedonic response to touch. These convey information about affective aspects of aversive touch and nociception. At the cortical level, primary somatosensory cortex (S1) remains the dominant entry

point for information carried along myelinated cutaneous pathways, with projections forming the sensory homunculus along the postcentral gyrus. There is evidence that integration of hedonic information into discriminatory touch representations in these early sensory structures occurs through centrally-mediated appraisal of pain and pleasure (Bushnell et al., 1999; Gazzola et al., 2012). This observation is consistent with the conventional view (Pessoa and Adolphs, 2010; Rolls, 2019) that affective modulation of sensory cortices results from feedback from central regions sensitive to hedonic value, including amygdala, prefrontal cortex (PFC) , anterior cingulate cortex (ACC) and insula (Ins). Yet, evidence for peripheral labeling of affective information suggests not all affective modulation of sensory signals is the result of central feedback (Qiu et al., 2006). Interestingly, while recent evidence has demonstrated that signals of hedonic and discriminative touch are integrated as early as the dorsal horn of the spinal cord (Abraira et al., 2017; Marshall and McGlone, 2020; Neubarth et al., 2020), the cortical instantiation of these signals does not appear to depend on this integration. For example, in patients lacking peripheral pathways for discriminatory touch (Aβ fiber), modulation of cortical activity by hedonic tactile signals (carried by C-fiber) is still observed in frontotemporal affect-related structures (Olausson et al., 2002; McGlone et al., 2014). It remains unknown the extent to which affective information from peripheral nociceptive receptors is represented in cortex as integrated with, versus dissociable from, non-hedonic tactile experience.

Anatomical projection studies in primates indicate information carried along unmyelinated C-fiber pathways does not project to the entirety of S1, as observed for A-fibers, but rather solely to an extreme anterior region of S1 (insula-adjacent area 3a; Whitsel et al., 2009; Vierck et al., 2013), with additional projections to Ins, ACC, and PFC (Baumgartner et al., 2006; Qiu et al., 2006). A meta-analysis of human neuroimaging studies identified a generalizable representation of physical pain (heat, mechanical, or visceral) in the ACC (Kragel et al., 2018). This pain signal is integrated with non-valenced sensory representations in the anterior Ins and ventromedial (vm) PFC (Visser et al., 2013). These data suggest that, despite the co-localization of A and C-fiber afferents in the skin, there are distinct brain regions that represent information carried by each. Determining the role of hedonic-labeled sensory signals for representing the environment necessitates further understanding of how they are represented in specific brain regions. The Ins (Craig, 2011, 2015) and ACC (Pollatos et al., 2016; Strigo and Craig, 2016), both cortical regions demonstrating sensitivity to hedonic-labeled information, are

often implicated in interoceptive sensation of the self, rather than exteroceptive experience of the external environment, whereas vmPFC acts to guide context-sensitive value-based decision making through the appraisal of affective signals and intrinsic motivations (Dixon et al., 2017; Hiser and Koenigs, 2018). Thus, if peripherally coded hedonic signals are not processed in the same manner as discriminatory touch — contributing to experiential discrimination of the external environment with predominant early projections to S1 — they may be processed as indicators of internal wellbeing, informative of homeostatic threat, to allow for prioritized responding to tactile harm.

Current views of the somatosensory representation of valenced information from the sensory surface are mostly based on examination of pain alone. While considerable research supports the neural bases of pain-coding in the periphery (McGlone and Reilly, 2010; Nagi et al., 2019), recent evidence indicates parallel C-tactile (CT) sensory fibers for caress or pleasant touch (Loken et al., 2009; Marshall et al., 2019). In this system, mechanoreceptors are found only in hairy skin and not on the glabrous (i.e., hairless) skin of the palms, where previous research had focused (McGlone and Reilly, 2010; McGlone et al., 2014; Marshall et al., 2019). These CT-fiber afferents respond more to pleasant soft brushes than neutral stimulation, and show the highest firing rates for stroking in speeds that are subjectively perceived as caress and are rated as most pleasant (Olausson et al., 2002; Loken et al., 2009; Croy et al., 2016). Thus, in the cutaneous system there are parallel dedicated receptors and labeled lines for aversive and appetitive forms of touch, reinforcing the notion that valence may be coded from the point of contact. As with C-fibers for aversive touch, information from dedicated pathways for pleasant touch modulates neural activity in the Ins and orbitofrontal cortices (OFC; Olausson et al., 2002; Rolls et al., 2003), as well as S1 (Gazzola et al., 2012); however, it is not known what specific contributions these regions make to the representation of pleasure.

Existing evidence from functional Magnetic Resonance Imaging (fMRI) indicating neural substrates of affective-tactile processing is based predominantly on study designs aimed at investigating either C- or CT-fiber pathways, but not both. These studies have also relied predominantly on univariate statistical approaches (Olausson et al., 2002; Loken et al., 2009; McGlone et al., 2014). The independent study of C- and CT-fibers does not allow for the dissociation between these two distinct systems and is unable to discriminate valence-specific

from general tactile salience and arousal. Relying on activation magnitude alone may miss important information that may distinguish tactile from hedonic features, especially if this information is represented by a population code in the somatosensory cortices (Chikazoe et al., 2014; Todd et al., 2020). Representational similarity analysis (RSA) allows examination of the similarity/dissimilarity of relationships between experimental conditions in an abstract and multidimensional representational space. By further decomposing patterns of neural activation into potential distinct representations of experience, one can examine neural activity as an integration of multiple heterogeneous sets of overlapping neural representations — as has been done recently to discriminate taste type from taste valence (Chikazoe et al., 2019). In the present study, we implemented an innovative analytic approach, *pattern component modelling* (PCM), which fits multiple theoretical similarity matrices characterizing perfect neural representation of information vectors, called here *information pattern components* (IPCs) to observed representational patterns extracted from a series of predefined regions of interest (ROIs).

Functional neuroimaging data was collected while participants received painful or pleasant tactile stimulation (Figure 1A) and viewed images of faces with neutral expressions. During this time, participants were instructed to focus on the visual stimuli rather than the tactile stimulation. RSA conducted on the BOLD signal identified the similarity/dissimilarity of tactile conditions that putatively stimulate distinct fiber pathways (Figure 1B). IPCs were created for task-relevant information constructs and included specific aspects of tactile experience (e.g., specific and non-specific touch, hedonic touch, etc.), and emotional experience (e.g., general trial valence, trial saliency etc.). Bayesian information criterion (BIC) analyses were then performed to characterize the combination of IPCs that best predicted observed similarity patterns of neural activity in each ROI. This allowed us to identify and weigh dissociable representations of discriminative and hedonic tactile signals, revealing potential C-fiber and CT-fiber pathways projection targets (See supplementary figure SF1 for a detailed schematic on PCM).

We predicted representation of the hedonic components of the tactile stimulation in frontotemporal cortices, including vmPFC, ACC and Ins, with little to no representation in sensory cortices. This would demonstrate the dual functionality of somatosensation and indicate that hedonic afferents genuinely reflect internal states rather than external sensory events. In addition, we expected that dissociable representational patterns for painful vs. pleasant tactile stimulation would be identified in the vmPFC and Ins, as prior neuroimaging analyses have

suggested that these regions may receive unprocessed information from hedonic-labeled lines. Patterns observed in the ACC were predicted to be most heavily weighted towards representation of aversive touch, consistent with this region's preferential activation in response to modality-general pain (Corradi-Dell'Acqua et al., 2016).
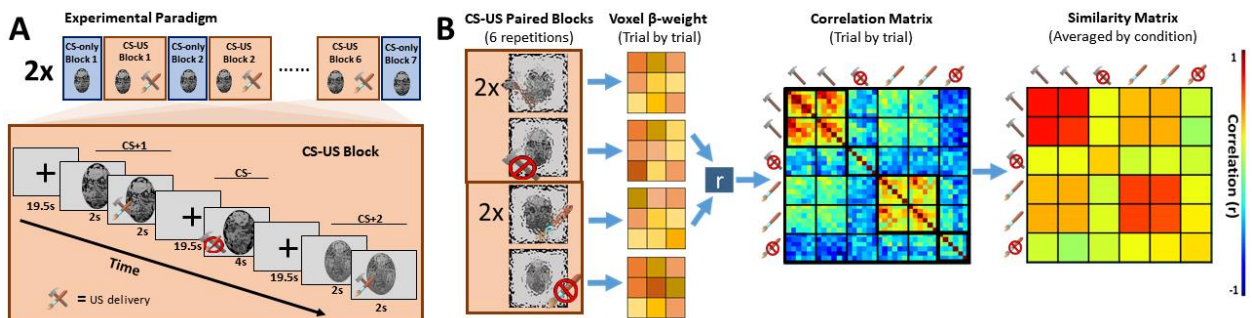

Figure 1. *A) Experimental time course.* Participants completed tactile visual conditioning tasks. Only data collected during CS-US paired blocked will be presented. *B) Representational similarity analyses (RSA).* RSA was conducted correlating all experimental trials independently. Resultant Pearson correlation coefficients were averaged across conditions (removing autocorrelation) to create a 6 x 6 condition similarity matrix comparing all conditions of interest.

Results

Results presented here focus on novel methodological approaches allowing for identification and weighting of independent sources of information represented in individual brain regions (i.e., PCM). For a visualization of traditional measures of representational distance between conditions, see Supplementary figure SF2.

IPC identification and weighting

Thirteen IPCs were constructed representing ideal categories of task-relevant information. As an example of the differences between these models, consider 'Specific touch [ST],' 'Non-specific touch [nST]' and 'Touch valence [TV]' (Table 1). Significant fit of an ST IPC would indicate that a region displayed a unique pattern of voxel-wise BOLD activation for each tactile experience encountered (i.e., appetitive touch, aversive touch and the absence of

both), while significant fit of nST would indicate that both salient tactile manipulations (i,e., appetitive and aversive touch) were being represented with high similarity to themselves and each other. Contrasting both these examples, model fit of TV would involve high representational similarity within appetitive and aversive trials, but dissimilarity between these two conditions, specifically placing the tactile valence on an opposing linear spectrum (Chikazoe et al., 2014). For a description of all thirteen IPCs, see Table 1 and for an extended description see Supplementary material S1.

To determine the IPC combinations that best explained the observed correlations in the data for each ROI, an uninformed *greedy best-first search* (*GBFS*) algorithm was used with Bayesian Information Criterion (BIC) analyses. The total number of paths required for a given search is defined as the n-path. This approach allowed for the decomposition of observed representational patterns into multiple unique contributing sources of information. Importantly, identified IPC combinations displayed better fit (i.e., lower BIC scores) to experimental data than of either a baseline model (predictor matrix of 1s) or the inclusion of all IPCs for all ROIs. For expanded detail on *GBFS* chains identified as most predictive for individual ROIs, see Supplementary Table ST1. To assess each IPC's independent contribution to the overall observed representational pattern for each ROI, multiple regressions were performed fitting the best performing combinations of IPCs (identified by the BIC analyses) as predictors to the observed data. The resultant regression coefficients (βs) indicated the proportional strength of each contributing IPC to the activational pattern observed in the ROIs. For complete summary, see Table ST2.

Analyses were conducted on nine non-overlapping ROIs; primary somatosensory cortex (S1) ; secondary somatosensory cortex (S2); primary/secondary visual cortex (combined as V1 hereafter); ventral visual structures (VVS); Amygdalae; ventromedial prefrontal cortex (vmPFC; Mackey and Petrides, 2014), anterior cingulate cortex (ACC) and separate anterior/posterior insular cortex (Ins) subdivisions (for rationale behind multiple insular ROIs, see Cauda et al., 2012). For additional details on defining our ROI see Supplementary Table ST2.

Somatosensory Cortices (S1): In S1, first level BIC analysis identified nST as the best individual fit to the S1 representational pattern. This fit was improved with the subsequent inclusion of 'Experimental task [ET]' and ST to the predictive model. IPC weighting identified

nST as the most strongly represented IPC in S1 ($\beta_{nST} = 0.129$) followed by ET ($\beta_{ET} = 0.056$) and ST ($\beta_{ST} = 0.039$). The three predictors explained 24.7 % of the variance ($R^2 = .247$, $F_{(3,1403)} = 154.39$, $p < .001$; Figure 2A). This ROI required two unique search paths to determine the best fitting IPC combination (n-path$_{S1} = 2$; see Supplementary Table ST3). This pattern indicates a representation of discriminative tactile experience rather than hedonic value in S1. In line of the dominant contralateral input to S1, and the lateralized tactile stimulation across tasks, two additional S1 PCM analyses were conducted in unilateral S1 ROIs. For full details on unilateral S1 analyses, see Supplementary materials S2. Interestingly, division of S1 into right and left hemispheric representational patterns suggests that the absence of hedonic information in S1 may be limited to positively valenced information carried along CT-fibre pathways. While right S1 represented the left lateralized specific touch experience (i.e., appetitive brushing and scanner-generic touch as distinct states), representational patterns in left S1 predicted by AP, lacking representation for right lateralized specific touch.

For S2, initial best fit was observed for nST. This fit was improved with additional inclusion of AP, ET and PE respectively. IPC weighting identified a similar pattern of representation, with nST the most strongly represented IPC S1 ($\beta_{nST} = 0.183$) followed by AP ($\beta_{AP} = 0.101$), ET ($\beta_{ET} = 0.040$) and PE ($\beta_{PE} = 0.030$). Together, these predictors accounted for 40.3 % of the variance ($R^2 = .403$, $F_{(3,1402)} = 238.00$, $p < .001$; Figure 2B). This suggests that S2 may receive hedonic signals that are not represented in S1.

Visual Cortices: Best model fits for both V1 and VVS representational patterns were found for the IPC ET. These fits did not improve with the inclusion of any additional IPCs. For V1, 2.1 % of the variance ($R^2 = .021$, $F_{(1,1405)} = 31.83$, $p < .001$) was explained by ET ($\beta_{ET} = 0.059$; Figure 2C), while in ventral visual structures, 2.6% of the variance ($R^2 = .026$, $F_{(2,1278)} = 38.83$, $p < .001$) was explained by this IPC ($\beta_{ET} = 0.061$; Figure 2D). This demonstrates that representational patterns in visual cortices are relatively uninformative of non-visual information, irrespective of its hedonic value.

Amygdalae: A combination of three IPCs best fit the representational pattern of bilateral amygdalae. These were, in order of identification, TV, nST, and ET. This combination of IPCs accounted for 12.0 % of the observed variance in the amygdalae ($R^2 = .120$, $F_{(3,1403)} = 64.97$, $p < .001$), with representational weights of $\beta_{TV} = 0.020$, $\beta_{nST} = 0.045$, and $\beta_{ET} = 0.033$ respectively

(Figure 3A). Notably, this is the only ROI to identify representation of valence on a linear spectrum, suggesting integration of positive and negative tactile signals prior to processing here.
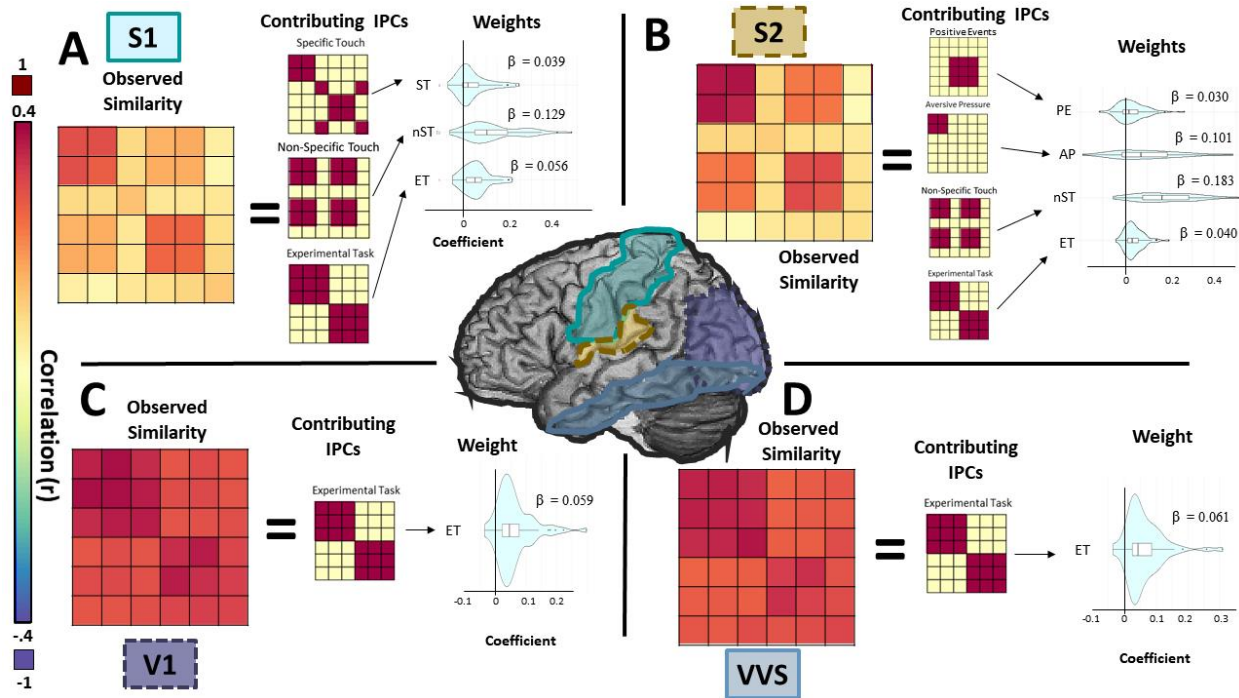

Figure 2. *Information pattern component in sensory cortices.* A) Representational similarity in primary somatosensory cortex (S1) was characterized by IPCs indicating representations of discriminatory touch, including non-specific tactile salience (nST), and specific tactile experience (ST). B) Representation of both hedonic and discriminative tactile signals were observed in S2, with strongest representation of nST and aversive pressure (AP). C/D) Similarity of representations in primary visual cortex (V1) and ventral visual structures (VVS) were characterized by intra-task similarity, consistent with the conservation of visual stimuli within experimental tasks.

Ventromedial Prefrontal Cortex: The vmPFC representational pattern was best fit to a combination of the IPCs 'Aversive pressure [AP]' and 'Appetitive brush [AB]' with weightings of $\beta_{AP} = 0.075$ and $\beta_{AB} = 0.052$. Total variance accounted for by these models was 7.5 % ($R^2 = .075$, $F_{(3,1404)} = 57.82$, $p < .001$). This demonstrates that vmPFC activity contains information about the hedonic value of the tactile stimulation, representing positive and negative value as distinctly independent signals (Figure 3B).

Anterior Cingulate Cortex: AP was identified as the initial IPC that best fit the ACC data with subsequent fit improvement from the sequential inclusion of nST and ET. Together, these predicted 18.4 % of the variance in this region ($R^2 = .184$, $F_{(3,1403)} = 106.70$, $p < .001$; Figure 3C). Specific strength of representations was found to be $\beta_{AP} = 0.062$, $\beta_{nST} = 0.058$, and $\beta_{ET} = 0.037$ respectively. This suggests that ACC represents general tactile information but is particularly sensitive to tactile information associated with pain.

Insula: The insula was anatomically subdivided at the anterior commissure into distinct non-overlapping anterior/posterior regions. Representational patterns in the anterior Insula (aIns) were best fit to a combination of four IPCs. In order of IPC identification, these were AP, nST, ET and NE. The pattern of activation in aIns was most heavily weighted by representation of AP ($\beta_{AP} = 0.12.6$), followed by nST ($\beta_{nST} = 0.044$), and ET ($\beta_{ET} = 0.028$). These explained 14.7 % of the variance ($R^2 = .147$, $F_{(4,1402)} = 61.33$, $p < .001$; Figure 3D).

A similar combination of IPCs best fit posterior Insula (pIns) representational patterns, though the order of identification, search requirement (n-path$_{pIns}$ = 3 vs. n-path$_{aIns}$ = 1; see Supplementary table ST3 for additional pIns paths), and presence of NE differed between regions. The order of IPC identification in pIns was nST, followed by ET then AP. This combination of IPCs was fitted to the observed data in pIns ($R^2 = .360$, $F_{(3,1403)} = 260.10$, $p < .001$; Figure 3E). The strongest IPC component in this region was nST ($\beta_{nST} = 0.112$), followed by AP ($\beta_{AP} = 0.070$), then ET ($\beta_{ET} = 0.047$). This shows that while the types of information processed in the insula may be similar across the anterior and posterior sections, the nature and weighting of these representations differ drastically.
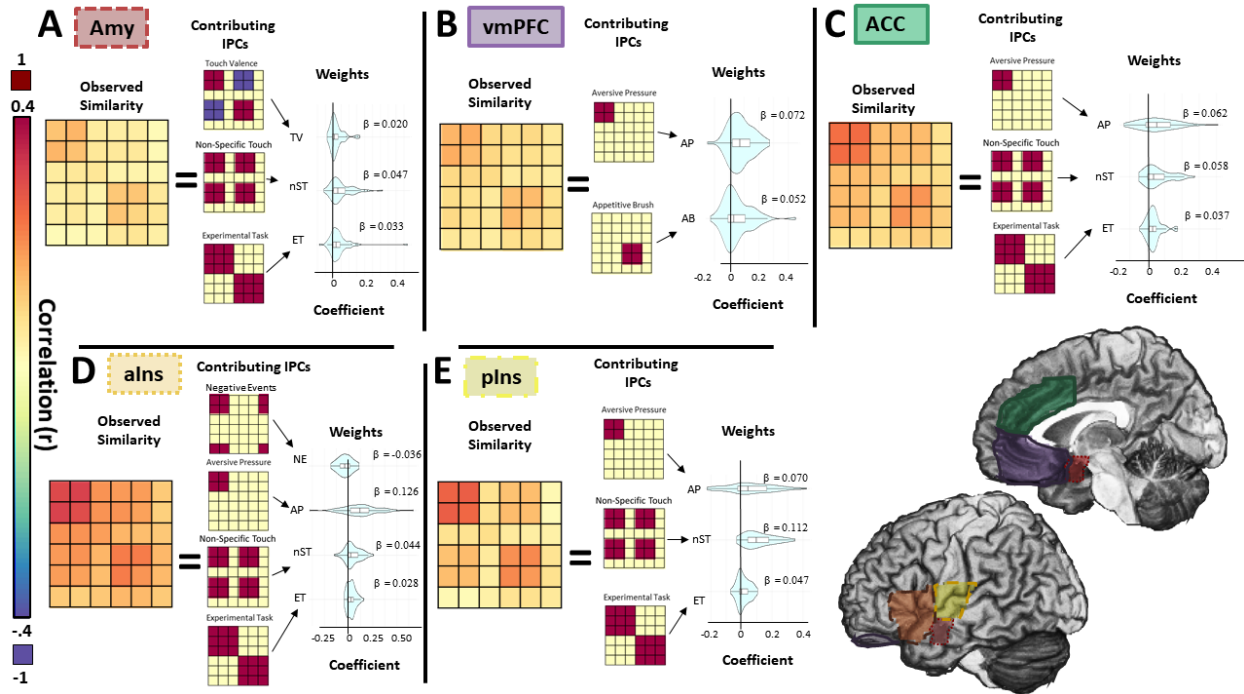
Figure 3. *Information pattern components in frontotemporal cortices.* A) Amygdalae displayed patterns of activation consistent with representations of a unidimensional hedonic-tactile spectrum (TV), as well as tactile saliency and general task effects. B) Activation patterns in vmPFC were unique, with representation of tactile pain and pleasure as dissociable contributing components. C/D/E) Anterior and posterior insula and ACC all displayed patterns of activation consistent with representation of tactile salience and painful sensation, though the specific biases for these types of information varied between the structures.

Cross-validation of results across brains

To ensure that regression fits were not a product of overfitting, we performed Monte-Carlo cross validation (CV) of our PCM on a randomly selected sample of participants (*'random-sample',* RS = 60), then fit these results as a predictor for held-out participants (the *'hold-out':* HO = 7). Specific outputs of interest included the proportion of CV iterations (i = 1000) in which an IPC was identified as a contributing component of the experimental data in the RS, and the model fit of the reconstructed data to the HO (Supplementary figure SF3). Proportion of iterations for IPC identification were compared to chance identification for each ROI (i.e., # of IPCs identified / total # of IPCs).

Overall, the similarity of IPC estimates generated from the Monte-Carlo CV to the whole sample data suggest a highly conserved pattern of representation across participants. Specifically, identical sets of IPCs to the full sample data were identified at a rate significantly above chance through Monte-Carlo CV for eight of the nine ROIs in RSs. The notable exception to this consistency was found in vmPFC: In addition to contributing IPCs identified in the full sample analyses (AP and AB), ET, nST and TA were also identified at a rate greater than chance. This suggests that while our PCM did accurately detect information consistently represented in vmPFC during our experimental paradigm - AP and AB representations were consistent - it may not reflect the extent of inter-participant variability of processing in this region. RS based on the specific participants in the HO resulted in the identification of three additional IPCs at a rate greater than chance suggesting that other information may be, but is not always, represented in this area. Furthermore, reconstructed models generated from the Monte-Carlo CV-identified IPCs in the RS were found to be significant predictors of the HO in seven of nine ROIs, with a minimum of β = 0.934. Reconstructed data from V1 and VVS failed to significantly predict the HO, indicating that these regions are less driven by information modeled in the current theorized pattern components. For complete summary of the cross-validation results, see Table 3.

To assess the robustness of IPC contributions, a one-way ANOVA was conducted on the average n-path data across iterations which identified a significant main effect of region ($F_{(8,7992)}$ = 195.507, p < .001). A follow-up series of independent sample t-tests (all reported p-values are Bonferroni-corrected) identified four distinct clusters of ROIs characterized by their n-path. A

lower search path likely indicates either a poor fit of the IPC models (if only a single model is frequently identified; e.g., V1/VVS), or robust representations for a specific subset of models (if identified IPC > 1; e.g. vmPFC). By contrast, a higher n-path likely indicates more overlapping representational space (e.g., insular subdivisions). Visual areas assessed required expansion of fewer paths than required by any other area (all $p < .001$), yet they did not differ significantly from each other ($p = 1.0$). Ventromedial PFC had more branching than either V1 or VVS but less than all other ROIs (all $p < 0.001$). ACC, amygdala, and S2 did not significantly differ from each other, yet required less expansion of search paths than S1 or either insular ROI. (all $ps < .001$). Finally, while aIns did not significantly differ from either pIns or S1 these other regions (both $ps = 1$), pIns displayed greater branching than S1 ($p < .001$). The greater n-path in these regions suggests that there is likely less distinct representational space for the IPC modeled in the current experiment.

Discussion

In this study we used pattern component modeling with representational similarity analysis to dissociate how discriminatory vs. hedonic tactile information, carried by A- and C-/CT-fibers respectively, contributes to population code representations in the human brain. Distinct representations of hedonic information were observed in frontal and temporal structures, including ventromedial prefrontal cortex (vmPFC), insula (Ins) and anterior cingulate cortex (ACC), as well as in secondary somatosensory cortex (S2). Importantly, primary somatosensory cortex (S1) did not represent all tactile information coded by peripheral receptors. No representation of positive hedonic touch signals carried by CT-fiber afferents was found. Visual areas, including primary/secondary visual cortex (V1) and ventral visual structures (VVS), displayed no representation of either affective, or discriminative touch information. By contrast, negative hedonic information made a minor contribution to representational patterns in S1 contralateral to the tactile stimulation (see Supplementary material S2), indicating that some nociceptive information may reach this area independent of frontotemporal processing. With respect to representational patterns in visual areas, it should be noted that while a single IPC (ET) was found to best fit similarity patterns in both visual areas, there were no consistently significant predictors identified in the MCCV analyses. This suggests that none of the modeled IPCs accurately described the signals generating the representations patterns observed in visual

areas; ET is the most predictive of the IPCs fitted, but likely not a true representation pattern in this area.

Together, the findings support the hypothesis that sensations carried by hedonic-labeled tactile signals - particularly those carried by CT-fiber pathways - may not be represented as discriminable signals in S1. Rather, this information is represented predominantly in frontotemporal structures more typically implicated in interoception (Craig, 2011; Pollatos et al., 2016; Strigo and Craig, 2016) and the central mediation of emotional relevance (McFarland and Sibly, 1975; Rolls, 2000; Todd et al., 2020). These findings indicate that hedonic tactile information for the most part does not contribute to representation of the external environment in the same fashion as discriminative touch information carried along A-fiber pathways. Of note, however, representation of aversive pressure in S1 contralateral to the tactile manipulation indicates that some nociceptive information does reach this area, though this representation likely includes both discriminatory and hedonic signals. This effect is consistent with evidence of pre-cortical integration of signals carried along A and C-fiber pathways at the dorsal horn (Abraira et al., 2017; Marshall and McGlone, 2020; Neubarth et al., 2020). Interestingly, similar integration and representation of signals carried along CT-fiber afferents is not observed, suggesting divergent projections for C and CT-fiber pathways. By demonstrating that hedonic signals of positive and negative tactile experience are represented as independent signals in frontotemporal structures yet mostly lack distinct representation in early sensory cortices, we provide a potential mechanism for the prioritized incorporation of this information into emotionally-guided cognitive processes.

Dissociable cortical representations for tactile information

Activation in S1 displayed representational patterns that discriminated different types of tactile experience, as well as *non-valence specific* components of tactile manipulations. The identification of representations for specific touch experiences (IPC: ST) in this area substantiates its traditional role in processing discriminatory tactile information as carried by out A-fiber afferents (McGlone and Reilly, 2010; McGlone et al., 2014). Note that nST is defined as containing a representational space for trials with no tactile manipulation (i.e., the tactile experience of lying in a scanner) of equal strength to those of the tactile manipulation. Thus, its manifestation cannot be generated by peripheral hedonic signalling, as these signals would not

inform this particular experience. Additionally, S1 strongly represented non-specific touch (IPC: nST). Though representations of nST may include information carried by C- and C-tactile fibers – this IPC includes perfect correlations for trials *within* both affective conditions – the defined similarity *between* the affective conditions in this IPC indicates that this information is unlikely to be in an unprocessed form. The two peripheral distinct signals are represented by overlapping activation patterns, potentially mediated by re-entrant projections of tactile salience from other frontotemporal structures (Vuilleumier, 2005; Pessoa and Adolphs, 2010). nST representation is likely either a discriminatory representation of body location (i.e., arm; not dependent on C- or CT- fiber activation) or general tactile salience (may or may not integrate information from C- and CT-fiber activation; i.e., hedonic salience). In support of the latter interpretation, there is evidence that S1 likely integrates re-entrant hedonic signals from multisensory emotion-related regions (Orenius et al., 2017).

Notably, IPCs indicating unprocessed projections of hedonic-labeled afferent pathways (i.e., IPCs Aversive pressure and Appetitive brush) were absent in bilateral representational patterns observed in this region, suggesting that these hedonic signals may not be instantiated in traditional somatosensory processing structures despite originating as external cutaneous sensation. Interestingly, unilateral investigation of left S1 did identify a representation pattern associated with aversive pressure (see Supplementary material S1), though this was observed in the absence of specific tactile discriminability (i.e., ST or rST). This suggests either that discriminative and nociceptive information are integrated prior to reaching S1 (for candidate regions, see Abraira et al., 2017; Marshall and McGlone, 2020; Neubarth et al., 2020), or alternatively, that sustained changes in tonic firing of rates of slow adapting mechanoreceptors (for review, see Knibestol, 1975; Abraham and Mathew, 2019) in response to the strong pressure manipulation (right hand) result in a tactile representation state in left S1 during CS- trials (pressure task) that is unique from the representation of scanner generic sensation (right hand) experienced during the brush manipulation (which was applied to the left hand). With substantive evidence to support both interpretations, it is likely that the observed IPC contributions reflect a combination of these processes. Importantly, however, there remains no evidence of unique representational patterns in S1 for signals of appetitive hedonic information carried by CT-fiber pathways.

Amongst all regions investigated, only vmPFC displayed independent representation of both appetitive and aversive touch (IPCs: AB/AP). This suggests that this region either A) receives information carried along C- and C-tactile fiber afferents as distinct signals prior to their integration with each other, or with other tactile information, or B) has decomposed an integrated hedonic representation back into distinct signals of positive and negative value to inform situation specific behaviours and decision. This dissociation is a striking contrast to recent observation of modality-general representations of hedonic valence in orbitofrontal cortices (OFC), which code valence along a unidimensional vector from pleasant to unpleasant (Miskovic and Anderson, 2018). One likely explanation for this divergent result is differences between studies in the definition of vmPFC ROIs. In the current study, we defined a mask that excluded the dorsal-most OFC structures (Brodmann area: BA 10). The choice to exclude this area was founded in cytoarchitectural differences between BA 10 and the rest of the vmPFC (Mackey and Petrides, 2014) — specifically, a substantial increase in granularity of its neurons (Barbas, 2015). Interestingly, activation in this region in response to pain stimuli has been demonstrated to involve *high-level processing* of the pain experience (Peng et al., 2018) and is proposed to create multimodal summaries of hedonic signals (Winecoff et al., 2013; Barrett, 2017). In contrast, agranular ventral prefrontal structures (conserved between OFC and the current vmPFC ROI) also display more category specific representation of experience (Miskovic and Anderson, 2018) and more direct autonomic control (Euston et al., 2012). Considering the critical role these ventral structures play in appraising emotional salience to guide value-based decision making (Euston et al., 2012; Dixon et al., 2017; Hiser and Koenigs, 2018), dissociable hedonic-labeled tactile representation in these regions may act as a mechanism to prioritize integration of action-outcomes into value appraisal to guide future decision-making processes.

Though distinct representation of appetitive touch was identified only in the vmPFC, distinct representations of aversive pressure were identified within the ACC as well as the anterior and posterior Ins. Notably, both of these regions are heavily implicated in the representation of painful experience (Corradi-Dell'Acqua et al., 2016; Kragel et al., 2018) and are postulated to underlie awareness of one's own internal homeostatic balance (Craig, 2011, 2015; Pollatos et al., 2016; Strigo and Craig, 2016), characterized as the *interoceptive self* (Craig, 2015). One potential explanation for this pattern of results is that hedonic-labeled peripheral afferents are not processed as tactile signals in the traditional view of sensation (Pinel

and Barnes, 2018; Gazzaniga et al., 2019). That is, they may not be instantiated in neocortex as representing the experience of contact with external objects in the environment. Rather, information carried along these pathways indicates internal concerns about homeostatic threat or social safety (Craig, 2011, 2015) and manifest cognitively as emotional feelings congruent with these states. Such patterns of representation demonstrate a potential dual function of proximal senses, consistent with Sherrington's classic distinction between exteroception and interoception: they represent not signals of the external world, but instead of the body itself, Sherrington's material "me" (Sherrington, 1906).

The utility of tactile receptors and peripheral afferents for interoceptive processes is potentially due to the proximal nature of tactile sensation. This is supported by recent work positing gustation an additional sensory contributor to interoceptive processing (Liman et al., 2014; Chikazoe et al., 2019), which offers another exemplar of a proximal sense with peripheral labelling of hedonic value (Liman et al., 2014).When an object is in direct contact with the senses, aversive sensation is likely informative of both the external environment and the organism's internal state (Craig, 2015). Information about the internal state acts as an immediate mechanism for motivating response independent of additional hedonic appraisal.

Mixed cortical representation of tactile information

Multiple structures displayed patterns of activity that indicated representation of C- and CT-fiber afferent information, though not in a mutually exclusive manner. Rather, representational patterns showed distinct similarity/dissimilarity between hedonic conditions, indicative of prior processing of this information. Specifically, in the ACC as well as the anterior and posterior Ins, patterns of neural activity were found to represent non-specific touch (IPC: nST) in addition to aversive pressure pain (IPC: AP). While the representation of nST is possibly dependent on information integrating both types of unmyelinated hedonic tactile afferents, the similarity of representation between the two valence manipulations indicate it is unlikely to be in an unprocessed form. The absence of distinct representation for pleasurable tactile signals in both the anterior and posterior Ins is particularly notable, as these regions have been highlighted as potential cortical recipients of C-tactile fiber information (Olausson et al., 2002; Rolls et al., 2003). While this may be due to variability in response to the appetitive touch manipulation used in the current design, the identification of a clear appetitive brush pattern component in the

vmPFC indicated that this is unlikely. Instead, this absence likely reflects the role of these regions in guiding both interoceptive and stimulus-guided attention (Han et al., 2019; Wang et al., 2019). Pain may be the more salient tactile signal for indicating the well-being of an organism, and thus given greater priority of resources. Furthermore, much of the prior work identifying modulation of Ins activity by pleasurable touch has been performed either independent of aversive touch (Olausson et al., 2002), or treating the two signals orthogonally without direct comparison (Rolls et al., 2003). This leaves open the possibility that results were driven by general affective salience of the tactile cue as observed currently, rather than the pleasurable sensation alone.

Interestingly, none of the anterior or posterior Ins, ACC, or vmPFC were found to display opposing representations of hedonic valence. However, in the amygdala, a clear representation of the hedonic experience of touch valence (IPC: TV) was observed. TV was represented as a single linear vector, with representations of appetitive brush anti-correlated to aversive pressure pain; the hedonic conditions represented as polar ends to a single valence spectrum: pleasure on one side and pain on the other. Thus, prior to its representation in the amygdala, tactile information once carried as unique signals along non-overlapping sensory afferents must be integrated into the same representational space. This is consistent with recent work in the olfactory domain demonstrating patterns of voxel-wise neural activity in this region as coding valence along a unidimensional vector from pleasant to unpleasant (Jin et al., 2015). Interestingly, however, corresponding bipolar representations have not been observed for either gustatory or visual hedonic information (Chikazoe et al., 2014, 2019). In light of this absence, the unidimensional valence spectrums observed previously in the olfactory domain, as well as in the current study, are likely indicating modality-specific hedonic processing rather than a centralized a-modal representation of emotional state (Miskovic and Anderson, 2018). In the current work in particular, this unidimensional hedonic vector may be related to the association of the tactile sensation with the concurrent visual stimuli rather than with the raw tactile signals in isolation, as multiple studies in both humans and non-human primates have implicated this region in guiding affect-biased attention (Todd et al., 2020) and emotional learning in vision (Morris et al., 1998; Everitt et al., 2003).

Conclusion

Somatosensation contains more information about the environment than traditionally believed. Beyond discriminative information pertaining to the identity of objects contiguous to ourselves, this system also signals the value of an object for our wellbeing; that is, the pain and pleasure of contact with it. In the current study, we use multivariate pattern component modeling to demonstrate that this hedonic tactile information is not processed in the same fashion as non-hedonic tactile information. The full spectrum of hedonic tactile information is not uniquely represented in primary somatosensory cortices but is represented in frontotemporal structures. Notably, representations of hedonic tactile information are observed in brain areas proposed to underlie the emergence of an interoceptive self. Thus, we propose that somatonsensory signals, originating from cutaneous mechanoreceptors through contact with the external world are not only critical for our exteroception – *feeling about the world around us* – but also interoception – *feelings about the world inside*.

Methods

Participants

Four-hundred and eighty-eight participants were recruited from Cornell University to complete an initial behavioural pilot assessment of affiliative responding to tactile stimulation. Of these, 107 participants ($\bar{x}_{age} = 21.1$, *sd* = 2.8; 41F) were recruited to complete the current study. We were unable to complete preprocessing of data for 40 participants: 27 participants had raw data corrupted related to server-transfer errors prior to preprocessing, for five we were unable to obtain convergence during the multi-echo independent component analysis (ICA), five did not have correct stimulus timing information, and three were excluded due to motion artifacts. Results from the remaining 67 participants are reported. All participants gave written, informed consent and had normal or corrected-to-normal vision. Participants were pre-screened for a history of anxiety and depression as well as other psychopathology, epilepsy and brain surgery. Pre-screening was followed up in person by an additional interview to ensure inclusion criteria were met. As this study was conducted as part of larger research program, all participants provided saliva samples for genotyping, and fecal sample for microbiome analyses. The

experiment was performed in accordance with the Institutional Review Board for Human Participants at Cornell University.

Stimuli and Apparatus

Three male and three female faces with neutral expressions were chosen from the Karolinska directed emotional faces picture set (Goeleven et al., 2008). These faces were used as conditioned stimuli (CS) in a classical conditioning paradigm. Unconditioned stimuli (US) consisted of either unpleasant, aversive pressure delivered to the right thumb, or a pleasurable, appetitive brush stroke to the participant's left forearm. These tactile manipulations were aimed to maximally activate C- and C-tactile somatosensory afferent respectively. Pressure-pain stimuli were delivered using a custom designed hydraulic device (Giesecke et al., 2004; Lopez-Sola et al., 2010) capable of transmitting controlled pressure to 1 cm^2 surface placed on the subjects' right thumbnail. Applied pressure levels were individually calibrated for each participant prior to the experiment to ensure that the pressure intensity was experienced as aversive but not excessively painful. Light appetitive brush strokes lasting ~4 s were manually applied to the left forearm by a trained experimenter to maximally activate CT-fiber pathways (McGlone et al., 2014). Individual subjective responses to brush stimuli were recorded in a separate session prior to scanning. Only participants from the initial behavioral experiment who had previously responded positively to the brush manipulation were invited to participant in the scanning session.

Procedure

While undergoing functional MR scanning, participants completed two separate conditioning tasks (appetitive conditioning and aversive conditioning), each involving a series of tactile and visual pairings (Figure 1A) (Visser et al., 2015). In each task, participants completed seven CS-only blocks interleaved with six CS-US paired blocks. Single blocks of either the CS-only or the CS-US pairing contained one presentation of each facial stimulus (i.e., 3 face stimuli per block of each conditioning task). Individual trials consisted of an initial fixation period (19500 ms) followed by the presentation of a face (4000 ms). A fixed and long interstimulus interval (19500 ms) was included in the experimental design to reduce intrinsic noise correlations and enable trial by trial analyses by means of RSA (Visser et al., 2013; Visser et al., 2016). During CS-only trials, all faces were presented without tactile stimulation. During CS-US

paired trials, two of three facial stimuli presentations overlapped with tactile stimulation, thus creating two CS+ and one CS-. The US was delivered from the midpoint of the face presentation (2000 ms post-onset), remained for the rest of the time the face was visible (2000 ms) and persisted following the offset (2000 ms; total US = 4000 ms). The order of face presentation was randomized within each CS-US paired block. Participants completed two experimental tasks (one for each US, order counterbalanced across participants), totaling 26 blocks (6 CS-US paired and 7 CS only blocks for each US type).

MRI Acquisition and Preprocessing

MR scanning was conducted on a 3 Tesla GE Discovery MR scanner using a 32-channel head coil. For each subject, a T1-weighted MPRAGE sequence was used to obtain high-resolution anatomical images (TR = 7 ms, TE = 3.42 ms, field of view (FOV) 256 x 256 mm, slice thickness 1 mm, 176 slices). Functional tasks were acquired with the following multi-echo (ME) EPI sequence: TR = 2000 ms, TE1 = 11.7 ms, TE2 = 24.2 ms and TE3 = 37.1 ms, flip angle 77°; FOV 240 x 240 mm. These parameters are consistent with recent work demonstrating improved effect-size estimation and statistical power for multi-echo acquisition parameters (Lombardo et al., 2016). Specifically, the multi-echo sequence was chosen due to its enhanced capacity for differentiating BOLD and non-BOLD signal (Kundu et al., 2012; Kundu et al., 2014), as well as its sensitivity for discrimination of small nuclei in areas susceptible to high signal dropout (Markello et al., 2018). A total of 102 slices was acquired with a voxel size of 3 x 3 x 3 mm. Pulse and respiration data were acquired with scanner-integrated devices.

Preprocessing and analysis of the fMRI data was conducted using Analysis of Functional NeuroImages software (AFNI; Cox, 1996) and the associated toolbox *meica.py* (Kundu et al., 2014; Kundu et al., 2017). For maximal sensitivity during multivariate pattern detection, no spatial smoothing was performed on the data (Haynes, 2015). Preprocessing of multi-echo imaging data followed the procedural steps outlined by Kundu et al. (Kundu et al., 2012; Kundu et al., 2013). An optimally combined (OC) dataset was generated from the functional multi-echo data by taking a weighted summation of the three echoes, using an exponential T2* weighting approach (Posse et al., 1999). Multi-echo principal components analysis (PCA) was first applied to the OC dataset to reduce the data dimensionality. Spatial independent components analysis (ICA) was then applied and the independent component time-series were fit to the pre-processed

time-series from each of the three echoes to generate ICA weights for each echo. These weights were subsequently fitted to the linear TE-dependence and TE-independence models to generate F-statistics and component-level κ and ρ values, which respectively indicate BOLD and non-BOLD weightings. The κ and ρ metrics were then used to identify non-BOLD-like components to be regressed out of the OC dataset as noise regressors. Regressor files of interest were generated for all individual trials across the experiment, modelling the time course of each stimulus presentation during each run (36 total events: 2 tasks X 6 CS-US blocks X 3 CS). The relevant hemodynamic response function was fit to each regressor for linear regression modeling. This resulted in a β coefficient and t value for each voxel and regressor. To facilitate group analysis, each individual's data were transformed into the standard brain space of the Montreal Neurological Institute (MNI).

fMRI Analyses: Structural Regions of Interest

To assess tactile (pressure *and* caress *and* non-specific touch) and hedonic (pressure *vs.* caress) representations in neural patterns, nine bilateral regions of interest (ROIs) were generated from the standard anatomical atlas (MNIa_caez_ml_18) implemented with AFNI. Selected ROIS were: Primary somatosensory cortex (S1), secondary somatosensory cortex (S2), primary/secondary visual cortex (V1), ventral visual structures (VVS), amygdala, ventromedial prefrontal cortex (vmPFC; Mackey and Petrides, 2014), anterior cingulate cortex (ACC) and separate posterior/anterior insula (Ins) divisions (consistent with its functional and histological divisions; for review, see Nieuwenhuys, 2012). S1 and V1 were selected as the primary sites of tactile and visual information respectively. VVS were chosen due to their role in visual classification (Kanwisher et al., 1997; Kravitz et al., 2013). Amygdala, vmPFC, ACC and posterior/anterior Ins divisions were selected for their hypothesized roles in affect (Anderson and Phelps, 2002; Chikazoe et al., 2014) and pain representations (Orenius et al., 2017; Kragel et al., 2018).

fMRI Analyses: RSA and Ideal Model Specification

In order to identify and compare the representational pattern elicited by the experimental conditions, representational similarity analysis (RSA; Mur et al., 2009; Kriegeskorte and Kievit, 2013; Figure 1B) was performed using the PyMVPA Python package (Hanke et al., 2009). For each participant, a vector was created containing the spatial patterns derived from β coefficients

from each voxel related to each particular event in each ROI. Pairwise Pearson coefficients were calculated between all vectors of a single ROI, thus resulting in a similarity matrix containing correlations for all trials for each participant (i.e., how closely the pattern of voxel activation elicited in one trial resembles the patterns of voxel activation observed in all other trials). Fisher transformations were performed on all similarity matrices to allow comparisons between participants. Correlation matrix transformations were performed using Matlab (The MathWorks, Natick, Massachusetts, USA) and BIC analyses were conducted in R (RCoreTeam, 2013).

Pattern component modelling (PCM; Kriegeskorte and Kievit, 2013; Diedrichsen et al., 2018) was performed using thirteen models of potential information pattern component (IPCs). These were generated to represent similarity matrices that would be observed in the experimental data if it were to contain perfect representation of distinct sources of information (see Supplementary material S1 for details). IPCs were constructed for 1) Experimental task, 2) Non-specific touch, 3) Specific touch, 4) Appetitive brush 5) Aversive pressure, 6) Touch valence, 7) Positive events, 8) Negative events, 9) All valence, 10) Salience, 11) Face Stimulus, 12) Violation of expectation, and 13) Temporal adjacency.

To determine the IPC combinations that best explained the observed correlations in the data for each ROI, we conducted Bayesian Information Criterion (BIC) analyses. As the IPCs identified in the current experiment contained some overlapping information, a regression of all potential IPCs would be insufficient to identify those most informative. To address this, a an uninformed *greedy best-first search* (*GBFS*) algorithm (Doran and Michie, 1966) was implemented to identify the best fitting IPC combination in a step wise manner (Supplementary figure SF1A). Initial model testing was conducted for each fitting of each independent IPC to the observed similarity for a given ROI (Level 1). Upon identification of the best fitting IPC (IPC$_{B1}$), model fitting was conducted on each remaining IPC in combination with IPC$_B$ (Level 2). The IPC combination (i.e., IPC$_{B1}$ + IPC$_{B2}$) that provided the best fit to the ROI data would be held as a constant for model fitting in Level 3. This process was repeated iteratively until no addition of remaining IPCs led to an improved fit to the ROI. A ΔBIC > 2 was defined as indicative of an improved fit (Fabozzi, 2014). Following similar equivalency criteria, all IPC combinations at a given search level with ΔBIC scores < 2 to the best fitting combination were also extended to path completion (Fabozzi, 2014).

fMRI Analyses: Cross-validation

Monte-Carlo cross-validation (CV; Picard and Cook, 1984) parameters were chosen to maximize CV performance by minimizing CV-variance while maximizing model selection accuracy (Arlot and Celisse, 2010). These analyses identified IPCs contributing to representational patterns for each ROI in the RS. Beta coefficients and intercepts, determined by fitting these IPCs as predictors to the experimental data, were used to create a reconstructed and averaged dataset. Model-improvement criterion and IPC-equivalency were handled in a manner identical to that described for the full-sample analyses. The reconstructed dataset was then fitted as a predictor to the HO, with each iteration approximating a single fold of a 10-fold validation.
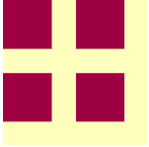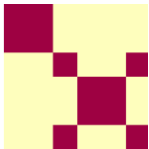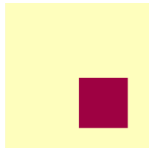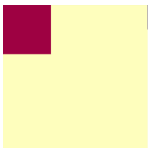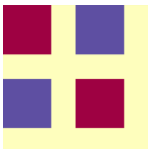
References
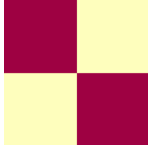
Abraham J, Mathew S (2019) Merkel Cells: A Collective Review of Current Concepts. Int J Appl Basic Med Res 9:9-13.

Abraira VE et al. (2017) The Cellular and Synaptic Architecture of the Mechanosensory Dorsal Horn. Cell 168:295-310 e219.

Anderson AK, Phelps EA (2002) Is the human amygdala critical for the subjective experience of emotion? Evidence of intact dispositional affect in patients with amygdala lesions. J Cogn Neurosci 14:709-720.

Arlot A, Celisse A (2010) A survey of cross-validation procedures. Statistical surveys 4:40-79.

Barbas H (2015) General cortical and special prefrontal connections: principles from structure to function. Annu Rev Neurosci 38:269-289.

Barrett LF (2017) The theory of constructed emotion: an active inference account of interoception and categorization. Soc Cogn Affect Neurosci 12:1-23.

Baumgartner U, Tiede W, Treede RD, Craig AD (2006) Laser-evoked potentials are graded and somatotopically organized anteroposteriorly in the operculoinsular cortex of anesthetized monkeys. J Neurophysiol 96:2802-2808.

Bushnell MC, Duncan GH, Hofbauer RK, Ha B, Chen JI, Carrier B (1999) Pain perception: is there a role for primary somatosensory cortex? Proc Natl Acad Sci U S A 96:7705-7709.

Cauda F, Costa T, Torta DM, Sacco K, D'Agata F, Duca S, Geminiani G, Fox PT, Vercelli A (2012) Meta-analytic clustering of the insular cortex: characterizing the meta-analytic connectivity of the insula when involved in active tasks. Neuroimage 62:343-355.

Chikazoe J, Lee DH, Kriegeskorte N, Anderson AK (2014) Population coding of affect across stimuli, modalities and individuals. Nat Neurosci 17:1114-1122.

Chikazoe J, Lee DH, Kriegeskorte N, Anderson AK (2019) Distinct representations of basic taste qualities in human gustatory cortex. Nat Commun 10:1048.

Corradi-Dell'Acqua C, Tusche A, Vuilleumier P, Singer T (2016) Cross-modal representations of first-hand and vicarious pain, disgust and fairness in insular and cingulate cortex. Nat Commun 7:10904.

Cox RW (1996) AFNI: software for analysis and visualization of functional magnetic resonance neuroimages. Computers and biomedical research, an international journal 29:162-173.

Craig AD (2011) Significance of the insula for the evolution of human awareness of feelings from the body. Ann N Y Acad Sci 1225:72-82.

Craig AD (2015) How do you feel? : an interoceptive moment with your neurobiological self. Princeton: Princeton University Press.

Croy I, Luong A, Triscoli C, Hofmann E, Olausson H, Sailer U (2016) Interpersonal stroking touch is targeted to C tactile afferent activation. Behav Brain Res 297:37-40.

Diedrichsen J, Yokoi A, Arbuckle SA (2018) Pattern component modeling: A flexible approach for understanding the representational structure of brain activity patterns. Neuroimage 180:119-133.

Dixon ML, Thiruchselvam R, Todd R, Christoff K (2017) Emotion and the prefrontal cortex: An integrative review. Psychol Bull 143:1033-1081.

Doran JE, Michie D (1966) Experiments with the Graph Traverser Program. Proceedings of the Royal Society of London A: Mathematical, Physical and Engineering Sciences 294:235-259.

Euston DR, Gruber AJ, McNaughton BL (2012) The role of medial prefrontal cortex in memory and decision making. Neuron 76:1057-1070.

Everitt BJ, Cardinal RN, Parkinson JA, Robbins TW (2003) Appetitive behavior: impact of amygdala-dependent mechanisms of emotional learning. Ann N Y Acad Sci 985:233-250.
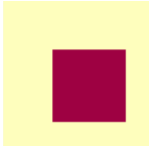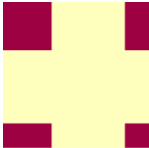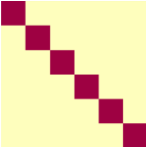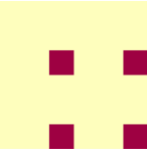
Fabozzi FJ (2014) The basics of financial econometrics : tools, concepts, and asset management applications. Hoboken, New Jersey: John Wiley & Sons, Inc.

Gazzaniga MS, Ivry RB, Mangun GR (2019) Cognitive neuroscience : the biology of the mind, Fifth edition. Edition. New York: W.W. Norton & Company.

Gazzola V, Spezio ML, Etzel JA, Castelli F, Adolphs R, Keysers C (2012) Primary somatosensory cortex discriminates affective significance in social touch. Proc Natl Acad Sci U S A 109:E1657-1666.

Giesecke T, Gracely RH, Grant MA, Nachemson A, Petzke F, Williams DA, Clauw DJ (2004) Evidence of augmented central pain processing in idiopathic chronic low back pain. Arthritis Rheum 50:613-623.

Goeleven E, De Raedt R, Leyman L, Verschuere B (2008) The Karolinska Directed Emotional Faces: A validation study. Cognition Emotion 22:1094-1118.

Han SW, Eaton HP, Marois R (2019) Functional Fractionation of the Cingulo-opercular Network: Alerting Insula and Updating Cingulate. Cereb Cortex 29:2624-2638.

Hanke M, Halchenko YO, Sederberg PB, Hanson SJ, Haxby JV, Pollmann S (2009) PyMVPA: A python toolbox for multivariate pattern analysis of fMRI data. Neuroinformatics 7:37-53.

Haynes JD (2015) A Primer on Pattern-Based Approaches to fMRI: Principles, Pitfalls, and Perspectives. Neuron 87:257-270.

Hiser J, Koenigs M (2018) The Multifaceted Role of the Ventromedial Prefrontal Cortex in Emotion, Decision Making, Social Cognition, and Psychopathology. Biol Psychiatry 83:638-647.

Iggo A (1959) Cutaneous heat and cold receptors with slowly conducting (C) afferent fibres. Q J Exp Physiol Cogn Med Sci 44:362-370.

Iggo A (1960) Cutaneous mechanoreceptors with afferent C fibres. J Physiol 152:337-353.

Jin J, Zelano C, Gottfried JA, Mohanty A (2015) Human Amygdala Represents the Complete Spectrum of Subjective Valence. J Neurosci 35:15145-15156.

Kanwisher N, McDermott J, Chun MM (1997) The fusiform face area: a module in human extrastriate cortex specialized for face perception. J Neurosci 17:4302-4311.

Knibestol M (1975) Stimulus-response functions of slowly adapting mechanoreceptors in the human glabrous skin area. J Physiol 245:63-80.

Kragel PA, Kano M, Van Oudenhove L, Ly HG, Dupont P, Rubio A, Delon-Martin C, Bonaz BL, Manuck SB, Gianaros PJ, Ceko M, Reynolds Losin EA, Woo CW, Nichols TE, Wager TD (2018) Generalizable representations of pain, cognitive control, and negative emotion in medial frontal cortex. Nat Neurosci 21:283-289.

Kravitz DJ, Saleem KS, Baker CI, Ungerleider LG, Mishkin M (2013) The ventral visual pathway: an expanded neural framework for the processing of object quality. Trends Cogn Sci 17:26-49.

Kriegeskorte N, Kievit RA (2013) Representational geometry: integrating cognition, computation, and the brain. Trends Cogn Sci 17:401-412.

Kryklywy JH, Ehlers MR, Anderson AK, Todd RM (2020) From Architecture to Evolution: Multisensory Evidence of Decentralized Emotion. Trends Cogn Sci.

Kundu P, Inati SJ, Evans JW, Luh WM, Bandettini PA (2012) Differentiating BOLD and non-BOLD signals in fMRI time series using multi-echo EPI. Neuroimage 60:1759-1770.

Kundu P, Santin MD, Bandettini PA, Bullmore ET, Petiet A (2014) Differentiating BOLD and non-BOLD signals in fMRI time series from anesthetized rats using multi-echo EPI at 11.7 T. Neuroimage 102 Pt 2:861-874.

Kundu P, Voon V, Balchandani P, Lombardo MV, Poser BA, Bandettini PA (2017) Multi-echo fMRI: A review of applications in fMRI denoising and analysis of BOLD signals. Neuroimage 154:59-80.

Kundu P, Brenowitz ND, Voon V, Worbe Y, Vertes PE, Inati SJ, Saad ZS, Bandettini PA, Bullmore ET (2013) Integrated strategy for improving functional connectivity mapping using multiecho fMRI. Proc Natl Acad Sci U S A 110:16187-16192.

Liman ER, Zhang YV, Montell C (2014) Peripheral coding of taste. Neuron 81:984-1000.

Loken LS, Wessberg J, Morrison I, McGlone F, Olausson H (2009) Coding of pleasant touch by unmyelinated afferents in humans. Nat Neurosci 12:547-548.

Lombardo MV, Auyeung B, Holt RJ, Waldman J, Ruigrok ANV, Mooney N, Bullmore ET, Baron-Cohen S, Kundu P (2016) Improving effect size estimation and statistical power with multi-echo fMRI and its impact on understanding the neural systems supporting mentalizing. Neuroimage 142:55-66.

Lopez-Sola M, Pujol J, Hernandez-Ribas R, Harrison BJ, Ortiz H, Soriano-Mas C, Deus J, Menchon JM, Vallejo J, Cardoner N (2010) Dynamic assessment of the right lateral frontal cortex response to painful stimulation. Neuroimage 50:1177-1187.

Mackey S, Petrides M (2014) Architecture and morphology of the human ventromedial prefrontal cortex. Eur J Neurosci 40:2777-2796.

Markello RD, Spreng RN, Luh WM, Anderson AK, De Rosa E (2018) Segregation of the human basal forebrain using resting state functional MRI. Neuroimage 173:287-297.

Marshall AG, McGlone FP (2020) Affective Touch: The Enigmatic Spinal Pathway of the C-Tactile Afferent. Neurosci Insights 15:2633105520925072.

Marshall AG, Sharma ML, Marley K, Olausson H, McGlone FP (2019) Spinal signaling of C-fiber mediated pleasant touch in humans. Elife 8.

McFarland DJ, Sibly RM (1975) The behavioural final common path. Philos Trans R Soc Lond B Biol Sci 270:265-293.

McGlone F, Reilly D (2010) The cutaneous sensory system. Neurosci Biobehav Rev 34:148-159.

McGlone F, Wessberg J, Olausson H (2014) Discriminative and affective touch: sensing and feeling. Neuron 82:737-755.

Miskovic V, Anderson AK (2018) Modality general and modality specific coding of hedonic valence. Curr Opin Behav Sci 19:91-97.

Morris JS, Ohman A, Dolan RJ (1998) Conscious and unconscious emotional learning in the human amygdala. Nature 393:467-470.

Mur M, Bandettini PA, Kriegeskorte N (2009) Revealing representational content with pattern-information fMRI--an introductory guide. Soc Cogn Affect Neurosci 4:101-109.

Nagi SS, Marshall AG, Makdani A, Jarocka E, Liljencrantz J, Ridderstrom M, Shaikh S, O'Neill F, Saade D, Donkervoort S, Foley AR, Minde J, Trulsson M, Cole J, Bonnemann CG, Chesler AT, Bushnell MC, McGlone F, Olausson H (2019) An ultrafast system for signaling mechanical pain in human skin. Sci Adv 5:eaaw1297.

Neubarth NL, Emanuel AJ, Liu Y, Springel MW, Handler A, Zhang Q, Lehnert BP, Guo C, Orefice LL, Abdelaziz A, DeLisle MM, Iskols M, Rhyins J, Kim SJ, Cattel SJ, Regehr W, Harvey CD, Drugowitsch J, Ginty DD (2020) Meissner corpuscles and their spatially intermingled afferents underlie gentle touch perception. Science 368.

Nieuwenhuys R (2012) The insular cortex: a review. Prog Brain Res 195:123-163.

Olausson H, Lamarre Y, Backlund H, Morin C, Wallin BG, Starck G, Ekholm S, Strigo I, Worsley K, Vallbo AB, Bushnell MC (2002) Unmyelinated tactile afferents signal touch and project to insular cortex. Nat Neurosci 5:900-904.

Orenius TI, Raij TT, Nuortimo A, Naatanen P, Lipsanen J, Karlsson H (2017) The interaction of emotion and pain in the insula and secondary somatosensory cortex. Neuroscience 349:185-194.

Peng K, Steele SC, Becerra L, Borsook D (2018) Brodmann area 10: Collating, integrating and high level processing of nociception and pain. Prog Neurobiol 161:1-22.

Pessoa L, Adolphs R (2010) Emotion processing and the amygdala: from a 'low road' to 'many roads' of evaluating biological significance. Nat Rev Neurosci 11:773-783.

Picard RR, Cook RD (1984) Cross-validation of regression models. Journal of the American Statistical Association 79.

Pinel JPJ, Barnes S (2018) Biopsychology, Tenth edition. Edition. Hoboken, NJ: Pearson Higher Education.

Pollatos O, Herbert BM, Mai S, Kammer T (2016) Changes in interoceptive processes following brain stimulation. Philos Trans R Soc Lond B Biol Sci 371.

Posse S, Wiese S, Gembris D, Mathiak K, Kessler C, Grosse-Ruyken ML, Elghahwagi B, Richards T, Dager SR, Kiselev VG (1999) Enhancement of BOLD-contrast sensitivity by single-shot multi-echo functional MR imaging. Magn Reson Med 42:87-97.

Qiu YH, Noguchi Y, Honda M, Nakata H, Tamura Y, Tanaka S, Sadato N, Wang XH, Inui K, Kakigi R (2006) Brain processing of the signals ascending through unmyelinated C fibers in humans: An event-related functional magnetic resonance imaging study. Cereb Cortex 16:1289-1295.

RCoreTeam (2013) R: A language and environment for statistical computing. In. Vienna, Austria.

Rolls ET (2000) Precis of The brain and emotion. Behav Brain Sci 23:177-191; discussion 192-233.

Rolls ET (2019) Emotion and reasoning in human decision-making. Economics-Kiel 13.

Rolls ET, O'Doherty J, Kringelbach ML, Francis S, Bowtell R, McGlone F (2003) Representations of pleasant and painful touch in the human orbitofrontal and cingulate cortices. Cereb Cortex 13:308-317.

Sherrington CS (1906) The integrative action of the nervous system. New York,: C. Scribner's sons.

Strigo IA, Craig AD (2016) Interoception, homeostatic emotions and sympathovagal balance. Philos Trans R Soc Lond B Biol Sci 371.

Todd RM, Miskovic V, Chikazoe J, Anderson AK (2020) Emotional Objectivity: Neural Representations of Emotions and Their Interaction with Cognition. Annu Rev Psychol 71:25-48.

Vallbo AB, Olausson H, Wessberg J (1999) Unmyelinated afferents constitute a second system coding tactile stimuli of the human hairy skin. J Neurophysiol 81:2753-2763.

Vierck CJ, Whitsel BL, Favorov OV, Brown AW, Tommerdahl M (2013) Role of primary somatosensory cortex in the coding of pain. Pain 154:334-344.

Visser RM, Scholte HS, Beemsterboer T, Kindt M (2013) Neural pattern similarity predicts long-term fear memory. Nat Neurosci 16:388-390.

Visser RM, Kunze AE, Westhoff B, Scholte HS, Kindt M (2015) Representational similarity analysis offers a preview of the noradrenergic modulation of long-term fear memory at the time of encoding. Psychoneuroendocrinology 55:8-20.

Visser RM, de Haan MI, Beemsterboer T, Haver P, Kindt M, Scholte HS (2016) Quantifying learning-dependent changes in the brain: Single-trial multivoxel pattern analysis requires slow event-related fMRI. Psychophysiology 53:1117-1127.

Vuilleumier P (2005) How brains beware: neural mechanisms of emotional attention. Trends in Cognitive Sciences 9:585-594.

Wang X, Wu Q, Egan L, Gu X, Liu P, Gu H, Yang Y, Luo J, Wu Y, Gao Z, Fan J (2019) Anterior insular cortex plays a critical role in interoceptive attention. Elife 8.

Whitsel BL, Favorov OV, Li Y, Quibrera M, Tommerdahl M (2009) Area 3a neuron response to skin nociceptor afferent drive. Cereb Cortex 19:349-366.

Winecoff A, Clithero JA, Carter RM, Bergman SR, Wang L, Huettel SA (2013) Ventromedial prefrontal cortex encodes emotional value. J Neurosci 33:11032-11039.

Table 1: *IPC* Glossary

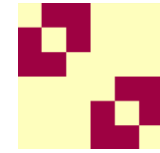| Name	Abbr.	Description	Visual Representation*
Experimental Task	*ET*	r = 1 for all comparisons between all trials in each conditioning task. • i.e., within conditioning tasks, CS+ has shared representation with CS-	
Non-Specific Touch	*nST*	r = 1 for all comparisons between all trials where a tactile manipulation occurred. • i.e., shared representation both within and between *APCS+ and **AVCS+.	
Specific-Touch	*ST*	r = 1 for all comparisons between all trials where an identical tactile experience occurred. • i.e., shared representation within, but not between APCS+, AVCS+ and CS- trials	
Appetitive Brush	*AB*	r = 1 for all comparisons between all trials that involved the delivery of an appetitive brush stroke to the participant's arm.	
Aversive Pressure	*AP*	r = 1 for all comparisons between all trials that involved the delivery of aversive pressure to the participant's thumb.	
Touch Valence	*TV*	r = 1 for all comparisons between CS+ trials within each conditioning task. r = -1 for all comparisons between CS+ trials between conditioning tasks. NOTE: This reflects a linear representation of hedonic *tactile* information.	

Positive Events	*PE*	r = 1 for all comparisons between all trials experienced as positively valenced relative to its experimental task. • i.e., $_{AP}$CS+ has shared representation with $_{AV}$CS-.	
Negative Events	*NE*	r = 1 for all comparisons between all trials experienced as negatively valenced relative to its experimental task. • i.e., $_{AV}$CS+ has shared representation with $_{AP}$CS-.	
All Valence	*AV*	r = 1 for all comparisons between trials containing positive events and between trials containing negative events. r = -1 for all comparisons between trials of positive events and negative events. *NOTE: This reflects a linear representation of *all* hedonic information.	

Salience	*Sa*	r = 1 for all comparisons between all trial with highly tactile salience.
		    • shared representation both within and between $_{AP}$CS+ and $_{AV}$CS+.
		r = 1 for all comparisons between all trial with minimal tactile salience
		    • shared representation both within and between $_{AP}$CS- and $_{AV}$CS-
		r = -1 for all correlation between highly and minimally salient trials	

Facial Stimulus	*FS*	r = 1 for all comparisons between trials where the visual stimulus presented (i.e., the face) was identical • i.e., distinct representation for each of the 6 CS (3CS X 2 Tasks)	
Violation of Expectation	*VE*	r = 1 for all comparisons correlation between all trials involving the less probable CS-US paired outcome NOTE: As there were two CS+ compared to one CS- for each experimental task, the less probable outcome was always the CS- trials	

Temporal Adjacency	*TA*	r = 1 for all comparisons between all comparisons that included trials that were temporally contained within the same block (i.e., temporally adjacent exposures).
		NOTE: Due to the removal of autocorrelation from within condition averaging, these did not contain temporally adjacent trials

Table 2: *IPC* coefficient weights*: Full sample*

ROI	Regression		Information Pattern Component weighting – β Coefficients												
	R^2	P value	ET	nST	ST	AB	AP	TV	PE	NE	AV	S	FS	VE	TA
S1	.247	2.8e-50	0.056	0.128	0.039	-	-	-	-	-	-	-	-	-	-
S2	.403	9.1e-88	0.040	0.183	-	-	0.101	-	-0.030	-	-	-	-	-	-
V1	.021	2.0e-8	0.059	-	-	-	-	-	-	-	-	-	-	-	-
VVS	.026	6.1e-10	0.061	-	-	-	-	-	-	-	-	-	-	-	-
Amy	.120	.00036	0.033	0.046	-	-	-	0.020	-	-	-	-	-	-	-
vmPFC	.075	8.9e-21	-	-	-	0.052	0.075	-	-	-	-	-	-	-	-
ACC	.184	1.1e-10	0.037	0.058	-	-	0.062	-	-	-	-	-	-	-	-
aIns	.147	8.2e-13	0.028	0.044	-	-	0.126	-	-	-0.036	-	-	-	-	-
pIns	.356	6.0e-66	0.047	0.112	-	-	0.070	-	-	-	-	-	-	-	-

Table 3: Cross Validation – Average values

ROI	Av. n-path	Information Pattern Component identification – % of Simulations (mean contributing β*; n = 55)													HO Fit (n = 6, df = 1,124)		
		ET	nST	ST	AB	AP	TV	PE	NE	AV	S	FS	VE	TA	R^2	P value	Recon. β
S1	1.934	100 (0.055)	100 (0.129)	60.2 (0.025)	0 -	19.9 -	18.8 -	7.8 -	0 -	4.5 -	0 -	0 -	0 -	0 -	.248	4.1e-5	0.978
S2	1.607	96.8 (0.041)	100 (0.185)	0 -	1.2 -	98.8 (0.094)	3.3 -	54.8 (0.002)	5.8 -	0 -	0 -	0 -	0 -	0 -	.411	1.5e-7	1.005
V1	1.212	100 (0.059)	0 -	0 -	0 -	0 -	0 -	0 -	0 -	0 -	0 -	0 -	0 -	0 -	.021	0.10	1.018
VVS	1.183	100 (0.061)	0 -	0 -	0 -	0.1 -	0 -	0 -	0 -	0 -	0 -	0 -	0 -	0 -	.028	0.07	1.022
Amy	1.539	85.0 (0.011)	83.4 (0.019)	0 -	20.9 -	22.1 -	75.2 (0.014)	0 -	0.5 -	0.3 -	1.3 -	0 -	0 -	4.7 -	.116	0.0049	0.988
vmPFC	1.327	28.6 (0.011)	34.9 (0.015)	0 -	65.2 (0.033)	65.7 (0.050)	6.3 -	0 -	0.8 -	0 -	0 -	0 -	0 -	23.1 (0.005)	.074	0.023	0.934
ACC	1.547	94.4 (0.034)	94.4 (0.055)	0 -	5.6 -	100 (0.067)	0 -	0 -	0.1 -	5.5 -	0 -	0 -	0 -	0 -	.191	0.00033	0.991
aIns	1.935	91.0 (0.029)	99.8 (0.050)	0 -	0.2 -	100 (0.107)	0 -	0 -	42.2 (0.16)	0 -	0 -	0 -	0 -	4.5 -	.153	0.0023	0.969
pIns	2.043	100 (0.043)	100 (0.102)	0 -	16.9 -	83.1 (0.059)	32.6 (0.009)	11.7 -	2.6 -	0 -	0 -	0 -	0 -	0 -	.363	4.5e-6	0.991

average βs are presented only for IPCs identified at a level significantly greater than chance (i.e., proportion of simulations IPC is identified > (Average # of contributing IPCs / Total IPCs))